

## TUNING SQUATTING CONTROLLERS FOR A HIP EXOSKELETON USING EMG-BASED BAYESIAN OPTIMIZATION

### Salvador Echeveste

Department of Mechanical and Industrial Engineering  
University of Illinois at Chicago  
Chicago, Illinois 60607  
Email: sechev6@uic.edu

### Akshay Subramanian

Department of Mechanical and Industrial Engineering  
University of Illinois at Chicago  
Chicago, Illinois 60607  
Adlai E. Stevenson High School  
Lincolnshire, IL 60069  
Email: akshay7d8@gmail.com

### Joshua Zatz

Department of Mechanical and Industrial Engineering  
University of Illinois at Chicago  
Chicago, Illinois 60607  
Email: jzatz2@uic.edu

### Pranav A. Bhounsule

Department of Mechanical and Industrial Engineering  
University of Illinois at Chicago  
Chicago, Illinois 60607  
Email: pranav@uic.edu

### ABSTRACT

Assistive exoskeletons offer potential benefits for mobility during dynamic activities such as squatting, yet tuning their controllers poses a significant challenge. Conventional methods based on manual adjustments or metabolic cost measurements are slow. We propose an EMG-based human-in-the-loop (HIL) optimization framework that integrates continuous EMG feedback into a Bayesian optimization algorithm to efficiently adjust the control parameters of a portable exoskeleton. In this pilot study (n=4), our approach achieves a 21.3% reduction in metabolic cost compared to a no-device condition and a 22.5% reduction relative to an unpowered exoskeleton, with the tuning process taking only 4 minutes and 40 seconds. Moreover, the method reduces muscle activation by up to 21.4% and improves perceived effort ratings. These results suggest that our strategy provides an efficient means for tuning exoskeleton controllers, with promising implications for mobility assistance and rehabilitation.

### INTRODUCTION

Squatting is a fundamental movement used in daily life and rehabilitation, requiring significant lower-limb strength and coordination. Assistive exoskeletons provide substantial support for load-bearing activities in rehabilitation. However, the effectiveness of these devices heavily depends on how well the control strategy is tuned to match the dynamic movements of the user. Improperly tuned controllers can lead to inefficient support, user discomfort, or even increased metabolic cost [1, 2]. Manual tuning of control parameters to suit individual users is time-consuming and impractical for real-world applications, especially considering the variability in user physiology [3].

Human-in-the-loop (HIL) optimization provides an effective solution to this challenge by automating the controller tuning process using physiological feedback from the user [4, 5]. Traditional HIL methods often rely on metabolic cost as a feedback signal for optimization, but this approach requires a particularly lengthy acquisition time to reach a steady-state measure [6, 7]. Each condition can take several minutes of data collection, significantly increasing the overall tuning duration.

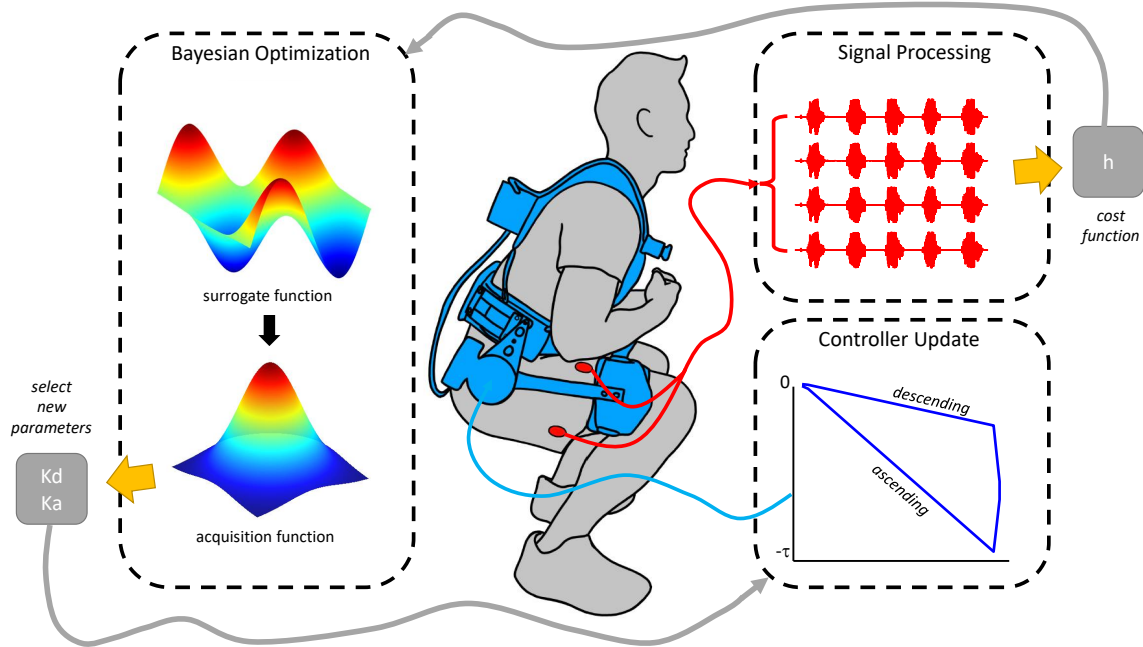


**FIGURE 1.** THIS FIGURE PRESENTS A COMPREHENSIVE DIAGRAM THAT DETAILS THE FLOW OF DATA WITHIN THE OPTIMIZATION SYSTEM. IT ILLUSTRATES HOW RAW EMG SIGNALS ARE ACQUIRED, PROCESSED, AND INCORPORATED INTO THE BAYESIAN OPTIMIZATION ALGORITHM, WHICH IN TURN ADJUSTS THE EXOSKELETON'S CONTROLLER PARAMETERS. KEY COMPONENTS OF THE FRAMEWORK, INCLUDING DATA ACQUISITION, SIGNAL PROCESSING, COST FUNCTION CALCULATION, AND PARAMETER TUNING, ARE CLEARLY DEPICTED.

To address this issue, we propose using surface electromyography (EMG) as an efficient physiological metric for tuning controllers in assistive exoskeletons. Unlike metabolic cost, EMG provides real-time feedback on muscle activation, enabling faster controller tuning and reducing the overall optimization time [4, 8]. By integrating EMG data into a Bayesian optimization framework, we demonstrate the ability to rapidly adjust controller parameters to reduce muscle effort and metabolic cost, achieving more efficient and personalized exoskeleton assistance. Preliminary results show a 22.7% reduction in metabolic cost compared to a no-device condition, with tuning completed in just 4 minutes and 40 seconds. This rapid EMG-based approach offers a scalable solution for optimizing assistive devices with various controller configurations for rehabilitation and daily use.

## RELATED WORKS

One of the main challenges in designing assistive exoskeletons is the variability in physiological responses between users, making it difficult to create universally optimal controllers [9, 10]. Manual tuning is often time-consuming and impractical, requiring expert intervention [3, 11]. HIL optimization emerges as a promising solution by automating the tuning process based on

user feedback [5, 12].

Traditionally, HIL methods rely on metabolic cost as a feedback signal, which reflects energy expenditure but requires extended data collection periods to reach steady-state measurements [6, 13]. This results in long optimization times, often exceeding 20 minutes [4], and is further complicated by the influence of external factors on metabolic readings [5].

Recent studies shift toward using faster physiological metrics such as EMG, which provides real-time feedback on muscle activation and allows for quicker controller adjustments [14, 15]. EMG-based HIL optimization shows promise in reducing tuning time and enhancing performance, especially in upper-limb exoskeletons [16, 17]. Its application in lower-limb exoskeletons is growing, though challenges with signal noise and consistency remain [18].

In walking exoskeletons, EMG integrated with HIL optimization demonstrates improvements in muscle effort reduction and gait mechanics [4]. Bayesian optimization techniques further refine this approach, effectively managing noisy physiological data and achieving faster tuning [8].

While EMG-based HIL optimization has been explored in walking, its use in load-bearing activities like squatting is limited [19]. Squatting requires precise control of movement and load distribution, presenting unique challenges. Our work ex-

tends this research by applying EMG-based HIL optimization to squatting, using Bayesian techniques to rapidly fine-tune stiffness controllers and improve metabolic cost efficiency.

In this work, we extend the advances by applying EMG-based HIL optimization to a hip exoskeleton designed specifically for squatting. By integrating EMG data into a Bayesian optimization framework, our method rapidly adjusts stiffness controllers to reduce muscle effort and metabolic cost. The novelty of this work lies in the efficiency of tuning with tuning completed in just 4 minutes and 40 seconds. This approach offers a scalable, efficient, and personalized solution for optimizing assistive exoskeletons in both rehabilitation and everyday settings. An overview of the procedure is shown in Fig. 1.

## METHODOLOGY

### System Overview

The system provides real-time hip assistance during squatting using an EMG-based HIL optimization framework. EMG signals from the user’s leg muscles adjust the exoskeleton’s stiffness, offering personalized support throughout the movement. The setup integrates a hip exoskeleton, EMG sensors, and a control algorithm based on Bayesian optimization. By assisting hip flexion and extension during squats, the system adapts to the user’s muscle activity, reducing effort and improving efficiency.



**FIGURE 2.** A DETAILED IMAGE OF THE HIP EXOSKELETON HIGHLIGHTING ITS PRINCIPAL FEATURES, INCLUDING THE 24V BLDC MOTOR FOR VARIABLE STIFFNESS CONTROL, ADJUSTABLE STRAPS FOR A SECURE FIT, AND RIGID PLASTIC BRACES. THE DESIGN IS OPTIMIZED TO SUPPORT HIP FLEXION AND EXTENSION DURING SQUATTING MOVEMENTS.

## Hip Exoskeleton Device

The exoskeleton (Fig. 2) assists hip flexion and extension during squatting via variable stiffness control that adapts resistance during both descent and ascent. It features a 24V BLDC (AK70-10 T) motor delivering 25 Nm peak and 8 Nm nominal torque, and is secured with adjustable shoulder, leg, and belt straps. Minimal rigid components (plastic braces and aluminum links) allow a range of motion from  $-30^\circ$  extension to  $90^\circ$  flexion.

Actuation is provided by a quasi-direct drive system with an open-loop torque controller that enables back-driveability for natural movement. A built-in motor encoder, reading at 1 MHz, captures hip angles at the joint center. Safety features include hard stops, two emergency stop buttons (one for torque cut-off and one for full shutdown), and continuous torque monitoring to prevent exceeding 25 Nm.

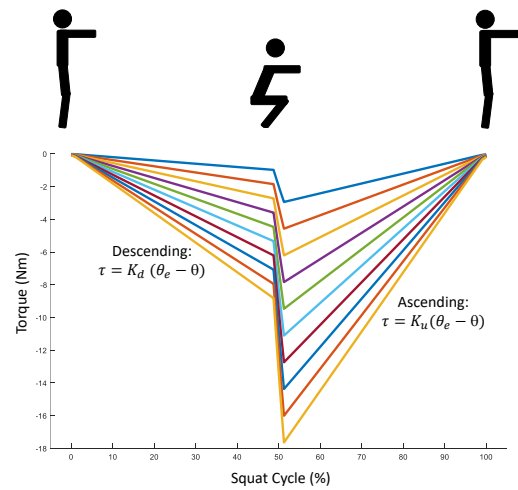


**FIGURE 3.** A SCHEMATIC REPRESENTATION OF THE EXOSKELETON’S CONTROL SYSTEM. THE HIGH-LEVEL CONTROLLER UTILIZES A FINITE STATE MACHINE (FSM) TO MANAGE FORWARD, BACKWARD, AND RESTING STATES, WHILE THE LOW-LEVEL CONTROLLER SENDS PRECISE TORQUE COMMANDS TO THE MOTOR ACCORDING TO THE SPECIFIED CONTROL LAW.

## Control Architecture

The control system operates on two levels: high-level control within Python 3.9.2 on a Raspberry Pi 4 and low-level control at the motor.

At the high level, the control system is structured around a finite state machine (FSM), which is chosen for its effectiveness in managing complex sequential operations and state transitions. The FSM comprises three principal states: forward leg move-

ment, backward leg movement, and a resting state. These states facilitate precise control of the leg swing dynamics by dividing leg swing control into forward and backward directions, managed separately by the FSM. Transitions between states are triggered by changes in angular velocity, allowing for responsive adjustments to movement patterns. To maintain natural movement dynamics, the controller aligns torque direction with velocity direction, ensuring positive work assistance. The control bandwidth is set at 350 Hz, a frequency selected to provide a balance between responsiveness and computational efficiency.

At the low level, high-level commands are transmitted via the CAN bus protocol to the integrated motor board, operating at 1M Hz. This quasi-direct open-loop architecture employs torque control to actuate the system. The choice of CAN bus communication ensures reliable and high-speed data transmission, crucial for real-time control.

### Stiffness Control Formulation

Stiffness control regulates the exoskeleton's resistance to movement, which is crucial for providing the right support during squatting. The goal is to provide enough resistance during the descent to control the user's motion, while allowing sufficient flexibility during the ascent to aid in standing back up. The control paradigm is illustrated in Fig. 3.

The control law for stiffness is based on a simplified linear spring model:

$$\tau = K(\theta_e - \theta) \quad (1)$$

Where:

- $\tau$  is the torque applied by the exoskeleton.
- $K$  is the stiffness coefficient, which is dynamically tuned.
- $\theta_e$  is the equilibrium joint angle (set to 0).
- $\theta$  is the normalized joint angle.

The stiffness coefficient  $K$  is different for ascending and descending. These values are tuned using EMG signals as feedback. A low stiffness value is applied during the descent to support controlled lowering, while the stiffness increases during the ascent to assist in standing up with minimal effort.

Figure 3 illustrates the controller design, what the torque profile looks like across different parameters.

### EMG Data

EMG sensors (Trigno, Delsys) are affixed to the rectus femoris and bicep femoris of each leg. EMG data are acquired at 1778 Hz, while angle orientation data are recorded at 148 Hz. Following sensor placement, the maximum voluntary contraction (MVC) of each muscle is determined and subsequently used for normalization.

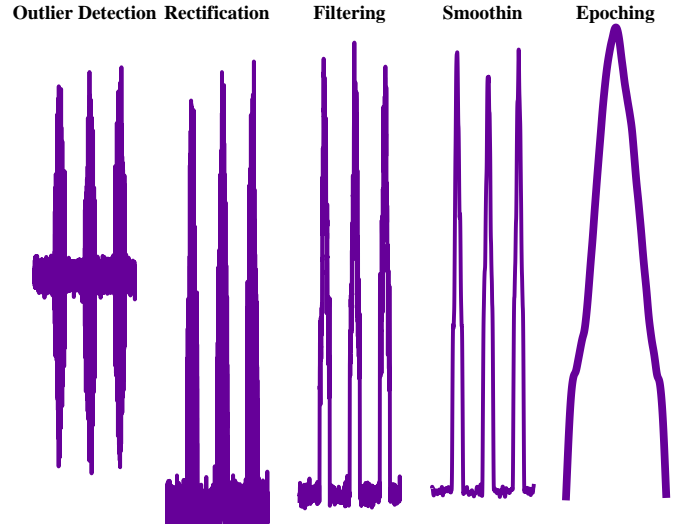


**FIGURE 4.** AN OVERVIEW OF THE EMG DATA PROCESSING WORKFLOW. RAW EMG SIGNALS ARE FILTERED, RECTIFIED, AND SMOOTHED, THEN NORMALIZED USING MVC VALUES. THESE PROCESSED SIGNALS ARE SUBSEQUENTLY USED TO COMPUTE COST FUNCTIONS CORRESPONDING TO THE FORWARD AND BACKWARD SWING PHASES DURING SQUATTING.

Each EMG signal is processed in MATLAB by applying a bandpass filter (20–450 Hz) to remove noise. Outliers, defined as values exceeding three standard deviations from the mean, are replaced using modified Akima cubic Hermite interpolation [20]. The signals are then rectified (by taking the absolute value and subtracting the DC offset) and smoothed using a moving maximum filter, a discretization filter, and a moving average filter. The window sizes for these filters (approximately 50 points for the maximum filter, bin sizes between 10 and 30 for the discretization filter, and up to 400 points for the moving average filter) are tuned individually to maximize the signal-to-noise ratio. Following smoothing, the signals are normalized by dividing by their corresponding MVC values. The EMG signal processing pipeline is summarized in Fig. 4, which details the filtering, rectification, smoothing, and normalization steps.

Angle data are linearly interpolated to match the EMG frequency and differentiated to obtain velocity, which is then used to segment the EMG signals into forward and backward swing datasets. These datasets are epoched and averaged to yield eight swing representations (four per movement direction). Two cost functions, one for forward ( $d = f$ ) and one for backward ( $d = b$ ) swings, are computed as:

$$h^d = \sum_{n=1}^4 \text{rms}(M_n^d), \quad (2)$$

where  $M_1^d, M_2^d, M_3^d, M_4^d$  denote the EMG signals from the respective muscles.

## Bayesian Optimization

Bayesian optimization is employed to identify the optimal parameter vector  $\mathbf{x} \in R^d$  that maximizes an unknown objective  $f: R^d \rightarrow R$ , using a Gaussian process (GP) surrogate model. The GP is defined by its mean function  $m(\mathbf{x})$  and covariance (kernel)  $k(\mathbf{x}, \mathbf{x}')$ , and for convenience we set  $m(\mathbf{x}) \equiv 0$ . Given a set of  $n$  evaluated inputs  $\mathbf{X} = [\mathbf{x}_1, \dots, \mathbf{x}_n]^\top$  and corresponding observations  $\mathbf{f} = [f(\mathbf{x}_1), \dots, f(\mathbf{x}_n)]^\top$ , the GP prior over  $\mathbf{f}$  is

$$p(\mathbf{f} | \mathbf{X}) = \mathcal{N}(\mathbf{f} | \mathbf{0}, \mathbf{K}), \quad (3)$$

where  $\mathbf{K} \in R^{n \times n}$  has entries  $K_{ij} = k(\mathbf{x}_i, \mathbf{x}_j)$ . For any set of  $n_*$  candidate test points  $\mathbf{X}_* = [\mathbf{x}_1^*, \dots, \mathbf{x}_{n_*}^*]^\top$ , the joint prior over observed outputs  $\mathbf{f}$  and latent values  $\mathbf{f}_* = [f(\mathbf{x}_1^*), \dots, f(\mathbf{x}_{n_*}^*)]^\top$  is

$$\begin{pmatrix} \mathbf{f} \\ \mathbf{f}_* \end{pmatrix} \sim \mathcal{N}\left(\mathbf{0}, \begin{pmatrix} \mathbf{K} & \mathbf{K}_* \\ \mathbf{K}_*^\top & \mathbf{K}_{**} \end{pmatrix}\right), \quad (4)$$

where  $\mathbf{K}_* \in R^{n \times n_*}$  with  $(\mathbf{K}_*)_{ij} = k(\mathbf{x}_i, \mathbf{x}_j^*)$ , and  $\mathbf{K}_{**} \in R^{n_* \times n_*}$  with  $(\mathbf{K}_{**})_{ij} = k(\mathbf{x}_i^*, \mathbf{x}_j^*)$ .

Conditioning on  $\mathbf{f}$ , the posterior predictive distribution for  $\mathbf{f}_*$  at  $\mathbf{X}_*$  is Gaussian:

$$p(\mathbf{f}_* | \mathbf{X}_*, \mathbf{X}, \mathbf{f}) = \mathcal{N}(\mathbf{f}_* | \boldsymbol{\mu}_*, \boldsymbol{\Sigma}_*), \quad (5)$$

with

$$\boldsymbol{\mu}_* = \mathbf{K}_*^\top \mathbf{K}^{-1} \mathbf{f}, \quad (6)$$

$$\boldsymbol{\Sigma}_* = \mathbf{K}_{**} - \mathbf{K}_*^\top \mathbf{K}^{-1} \mathbf{K}_*, \quad (7)$$

where  $\boldsymbol{\mu}_* \in R^{n_*}$  is the vector of posterior means and  $\boldsymbol{\Sigma}_* \in R^{n_* \times n_*}$  the posterior covariance. For a single test point  $\mathbf{x}$ , we write  $\boldsymbol{\mu}(\mathbf{x})$  for its predictive mean and  $\sigma^2(\mathbf{x})$  for the corresponding variance (i.e. the diagonal entry of  $\boldsymbol{\Sigma}_*$ ).

We employ the ARD Matérn 5/2 kernel:

$$k(\mathbf{x}, \mathbf{x}') = \sigma_f^2 \left(1 + \sqrt{5}r + \frac{5}{3}r^2\right) \exp(-\sqrt{5}r), \quad (8)$$

where the scaled distance  $r$  is defined as

$$r = \sqrt{\sum_{i=1}^d \frac{(x_i - x'_i)^2}{\ell_i^2}}. \quad (9)$$

Here  $d$  is the input dimension,  $\sigma_f^2$  the signal variance, and  $\ell_i$  the length-scale for the  $i$ th input.

To select the next evaluation, we maximize the Expected Improvement (EI) acquisition function. Let  $f_{\text{best}} = \max_{1 \leq i \leq n} f(\mathbf{x}_i)$  be the best observed value and  $\xi \geq 0$  an exploration parameter. For a candidate  $\mathbf{x}$ ,

$$\text{EI}(\mathbf{x}) = (\boldsymbol{\mu}(\mathbf{x}) - f_{\text{best}} - \xi) \Phi(Z) + \sigma(\mathbf{x}) \phi(Z), \quad (10)$$

$$Z = \frac{\boldsymbol{\mu}(\mathbf{x}) - f_{\text{best}} - \xi}{\sigma(\mathbf{x})}, \quad (11)$$

where  $\Phi(\cdot)$  and  $\phi(\cdot)$  are the standard normal CDF and PDF, respectively. The next query is

$$\mathbf{x}_{n+1} = \arg \max_{\mathbf{x} \in \mathcal{X}} \text{EI}(\mathbf{x}), \quad (12)$$

with  $\mathcal{X} \subseteq R^d$  the feasible domain.

## Experimental Protocol

The study is approved by the University of Illinois at Chicago Institutional Review Board (STUDY 1022-2022). A one-day protocol is conducted with four healthy participants (age:  $24.75 \pm .83$  years; weight:  $60.9 \pm 5.9$  kg; height:  $172.5 \pm 10.6$  cm, male: 4, female: 0). Subjects perform squats while the exoskeleton assists with hip flexion and extension. The protocol consists of three phases: acclimation, tuning, and validation. During acclimation, participants perform squats under all three conditions to familiarize themselves with the device. During tuning, the stiffness of the exoskeleton is adjusted using EMG-based HIL optimization. Finally, in the validation phase, optimal stiffness settings are used to evaluate performance over a sustained period. The participants perform squats under three conditions: no exoskeleton, unpowered exoskeleton, and powered exoskeleton. To validate the optimal controller, metabolic cost measurements are collected for 2 minutes for each condition using a COSMED K5. The data is then used to estimate energy expenditure using instantaneous cost mapping [21].

The experiment lasts approximately three hours, with frequent rest breaks to prevent fatigue. A summary of the experimental protocol is shown in Table 1.

## RESULTS

We evaluate the impact of EMG-based HIL optimization on metabolic cost during squatting. The optimized exoskeleton reduces metabolic cost by 21.3% compared to no device and by

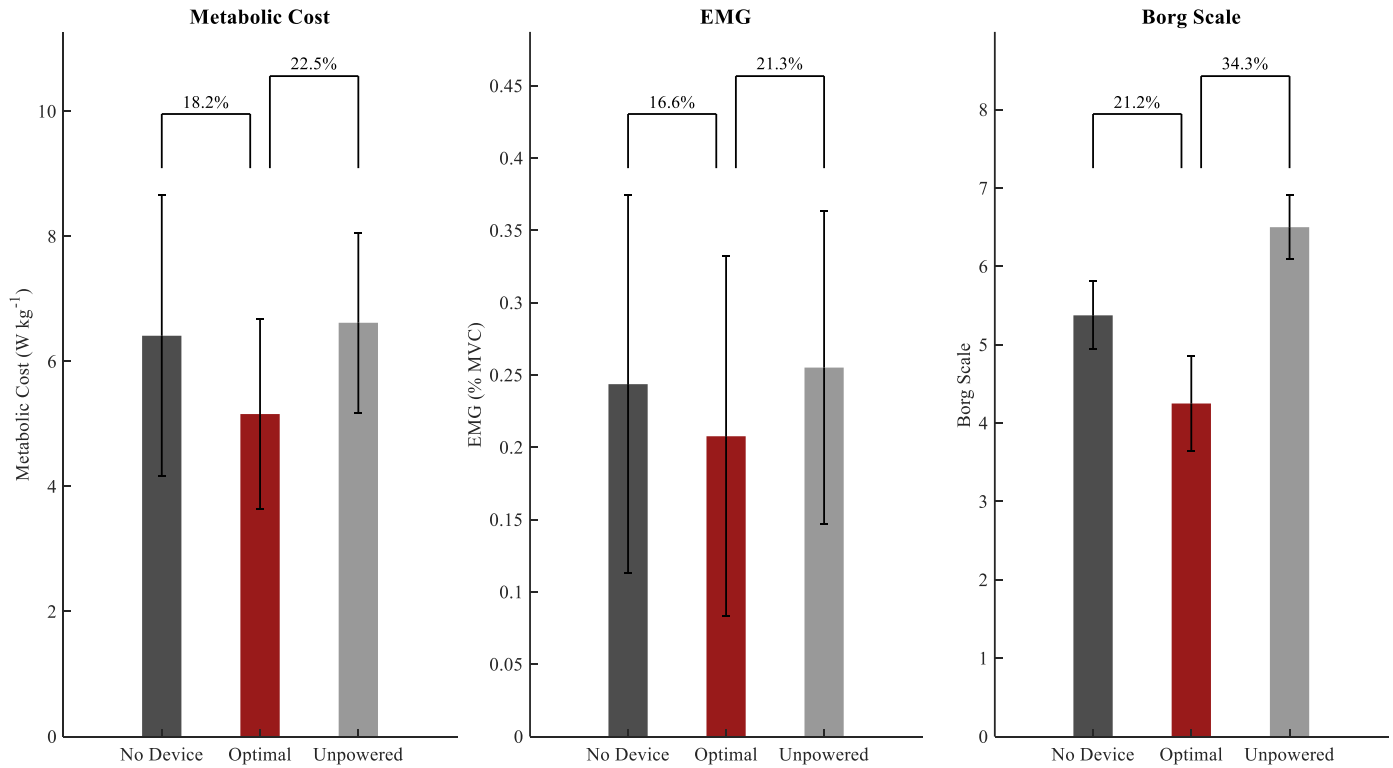


**FIGURE 5.** A BAR GRAPH COMPARING KEY PERFORMANCE METRICS—METABOLIC COST, MUSCLE EMG ACTIVITY, AND SUBJECTIVE BORG SCALE RATINGS—ACROSS THREE CONDITIONS: NO EXOSKELETON, UNPOWERED EXOSKELETON, AND OPTIMIZED CONTROLLER. PERCENTAGE REDUCTIONS ACHIEVED WITH THE OPTIMIZED CONTROLLER ARE SHOWN, WITH ERROR BARS REPRESENTING STANDARD DEVIATIONS.

**TABLE 1.** EXPERIMENTAL PROTOCOL SUMMARY

Phase	Segment	Conditions/Trials	Duration	Rest Time
<b>Acclimation</b>	No Device Activity	3 Conditions	20s	45s
	Unpowered Device	3 Conditions	20s	45s
	Powered Device	3-6 Conditions	20s	45s
<b>Tuning Phase</b>	Initialization	4 Trials	20s	45s
	Tuning	10 Trials	20s	45s
<b>Validation</b>	No Device	1 Condition	2 min	5 min
	Unpowered Device	1 Condition	2 min	5 min
	Optimal Assistance	1 Condition	2 min	5 min

22.5% compared to an unpowered exoskeleton (Fig. 5). These improvements underscore the benefits of real time controller tuning on energy efficiency and user performance.

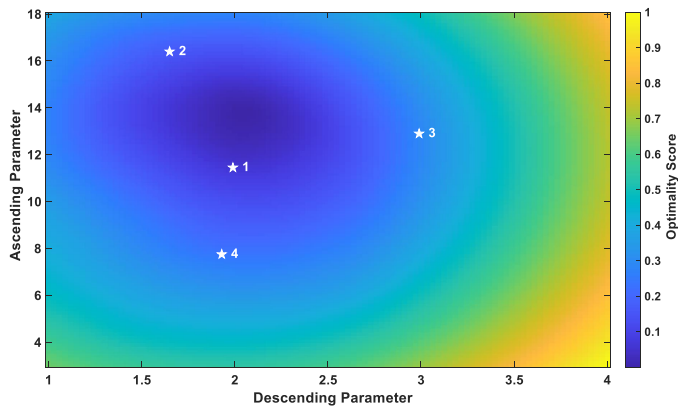
Figure 6 shows a heat map of control parameters and their associated cost function values for all subjects. The map clearly delineates regions where the cost function is minimized, with

stars marking the optimal settings. This visualization confirms the convergence of the Bayesian optimization process and illustrates that controller performance is highly sensitive to parameter variations. Although individual physiology varies, the framework reliably identifies efficient parameter sets across subjects.

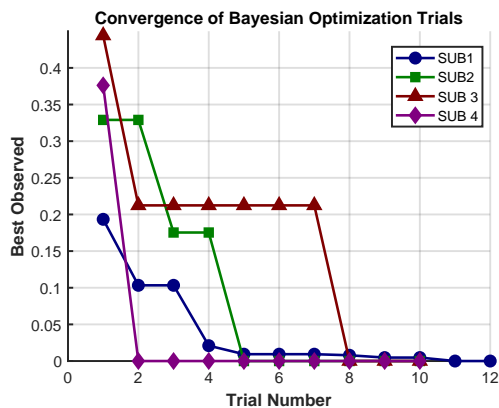
Figure 7 plots the best normalized cost function value at each trial for every subject. The consistent downward trend observed in the plots indicates that the Bayesian optimization algorithm quickly converges to effective control parameters. This rapid convergence is critical for practical applications where tuning must occur in real time.

Figure 8 presents detailed kinematic profiles of simulated squat motions. The subplots display joint angles, angular velocity, control torque, and power output as functions of the normalized squat phase. These profiles reveal that the exoskeleton dynamically synchronizes its assistance with the user’s movement during both the descent and ascent phases, thereby improving movement efficiency.

Subjective feedback on perceived effort is also collected using a Borg scale (ranging from 1 for very poor to 10 for excel-



**FIGURE 6.** A HEAT MAP DEPICTING THE RELATIONSHIP BETWEEN VARIOUS CONTROL PARAMETER COMBINATIONS AND THEIR CORRESPONDING COST FUNCTION VALUES ACROSS ALL SUBJECTS. OPTIMAL PARAMETER SETS ARE HIGHLIGHTED WITH STARS, EMPHASIZING THE SETTINGS THAT ACHIEVED THE MINIMUM COST FUNCTION VALUE DURING THE BAYESIAN OPTIMIZATION PROCESS.



**FIGURE 7.** CONVERGENCE PLOTS FOR EACH SUBJECT SHOWING THE NORMALIZED BEST COST FUNCTION VALUE FOUND AT EVERY TRIAL. THE GRAPHS DEMONSTRATE THE RAPID CONVERGENCE OF THE OPTIMIZATION ALGORITHM TOWARD EFFECTIVE CONTROL PARAMETERS FOR ALL SUBJECTS.

lent). Participants rate the optimized exoskeleton with an average score of 4.25, which is notably lower than the scores for the unpowered device (6.5) and no device (5.36). This reduction in perceived effort complements the objective metabolic improvements observed.

Finally, the optimized controller reduces average EMG activity across four muscles by 16.6% relative to no device and by 21.4% compared to the unpowered condition. This decrease in

muscular activity further supports the effectiveness of the tuning approach in reducing the physical effort required during squatting.

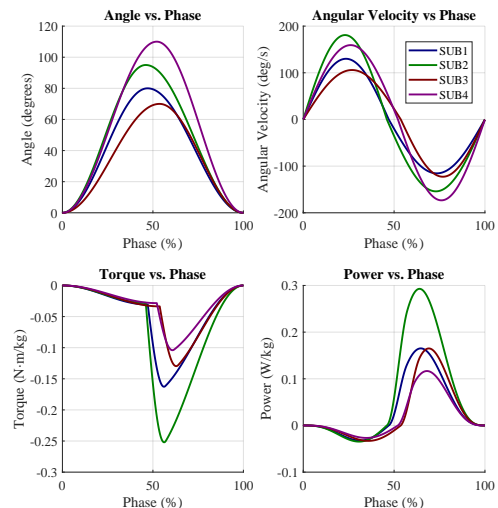


**FIGURE 8.** DETAILED KINEMATIC PROFILES FOR FOUR SUBJECTS DURING SQUATTING, PRESENTED AS FOLLOWS: (A) JOINT ANGLE (DEGREES) VERSUS NORMALIZED SQUAT PHASE (B) ANGULAR VELOCITY (DEG/S) VERSUS SQUAT PHASE, (C) CONTROL TORQUE (N·M/KG) VERSUS SQUAT PHASE, AND (D) POWER (W/KG) VERSUS SQUAT PHASE. THESE PROFILES ILLUSTRATE HOW THE EXOSKELETON'S ASSISTANCE SYNCHRONIZES WITH THE USER'S MOVEMENT THROUGHOUT THE SQUAT CYCLE.

## DISCUSSION

This study demonstrates that EMG-based HIL optimization improves exoskeleton stiffness control during squatting. The optimized controller achieves significant metabolic cost reductions (21.3% relative to no device and 22.5% relative to an unpowered exoskeleton) while completing the tuning process in just 4 minutes and 40 seconds. This efficiency makes the method a strong alternative to conventional metabolic cost based tuning approaches.

In addition to metabolic improvements, the controller tuning also decreases EMG activity (by 16.6% compared to no device and 21.4% compared to the unpowered condition) and lowers perceived effort (with an average rating of 4.25 compared to higher ratings for the other conditions). These findings indicate that the optimized exoskeleton not only reduces energy expenditure but also improves muscle coordination and user comfort.

A noteworthy advantage of our approach is its rapid convergence. The EMG-based Bayesian optimization reaches optimal control parameters in a fraction of the time (4 minutes and 40 seconds) compared to the 15.8 minutes required by traditional metabolic cost based methods [19]. This acceleration minimizes the tuning duration and reduces participant fatigue, thereby enhancing the practical applicability of the method for real time, personalized tuning.

The heat map in Figure 6 offers valuable insight into the control parameter space. It clearly identifies regions where the cost function is minimized, indicating that the optimization process effectively navigates parameter variations even in the presence of individual differences. The convergence plots in Figure 7 further confirm the reliability and stability of the tuning process across subjects.

Kinematic profiles in Figure 8 reveal that the controller tuning aligns the exoskeleton's assistance with the natural motion phases of squatting. The correspondence between control torque, power output, and the squat phase demonstrates that the tuning process enhances movement efficiency while reducing metabolic cost.

While these results are promising, the study has limitations. The small sample size and potential variability in EMG sensor placement and signal processing may affect generalizability. Future work will focus on refining sensor calibration, incorporating additional physiological metrics, and validating the approach on a larger and more diverse population.

Overall, the findings support that EMG-based HIL optimization enhances exoskeleton performance by reducing metabolic cost, lowering muscle activation, and improving user comfort. The rapid convergence and personalized tuning capabilities underscore the potential of this method for assistive and rehabilitative applications.

## CONCLUSION

This study demonstrates that EMG-based Bayesian optimization is a rapid and effective method for tuning exoskeleton controllers during squatting. The optimized tuning significantly reduces metabolic cost, improves user comfort, and lowers perceived effort. With the entire process completing in just 4 minutes and 40 seconds, this approach supports real time, personalized adjustments for both rehabilitation and daily use.

By integrating EMG data into a Bayesian framework, the method provides physiological feedback that facilitates adaptive control. This efficient approach offers a clear advantage over traditional metabolic cost based tuning methods and improves the interaction between the user and the exoskeleton. Future work will focus on enhancing the optimization process by incorporating additional physiological signals, refining sensor calibration, and testing the method on a larger scale. Overall, EMG-based Bayesian optimization presents a promising advance in assistive

technology, with the potential to significantly improve exoskeleton performance and user satisfaction.

## REFERENCES

- [1] Collins, S. H., Wiggin, M. B., and Sawicki, G. S., 2015. "Reducing the energy cost of human walking using an unpowered exoskeleton". *Nature*, **522**(7555), June, pp. 212–215.
- [2] Mooney, L. M., Rouse, E. J., and Herr, H. M., 2014. "Autonomous exoskeleton reduces metabolic cost of human walking during load carriage". *Journal of NeuroEngineering and Rehabilitation*, **11**(1), May, p. 80.
- [3] Quesada, R. E., Caputo, J. M., and Collins, S. H., 2016. "Increasing ankle push-off work with a powered prosthesis does not necessarily reduce metabolic rate for transtibial amputees.". *Journal of biomechanics*, **49**(14), Oct., pp. 3452–3459. Place: United States.
- [4] Zhang, J., Fiers, P., Witte, K. A., Jackson, R. W., Poggensee, K. L., Atkeson, C. G., and Collins, S. H., 2017. "Human-in-the-loop optimization of exoskeleton assistance during walking". *Science*, **356**(6344), pp. 1280–1284. eprint: <https://www.science.org/doi/pdf/10.1126/science.aal5054>.
- [5] Ferris, D. P., Sawicki, G. S., and Daley, M. A., 2007. "A PHYSIOLOGIST'S PERSPECTIVE ON ROBOTIC EXOSKELETONS FOR HUMAN LOCOMOTION.". *International journal of HR : humanoid robotics*, **4**(3), Sept., pp. 507–528. Place: United States.
- [6] Selinger, J. C., and Donelan, J. M., 2014. "Estimating instantaneous energetic cost during non-steady-state gait.". *Journal of applied physiology (Bethesda, Md. : 1985)*, **117**(11), Dec., pp. 1406–1415. Place: United States.
- [7] Handford, M. L., and Srinivasan, M., 2016. "Robotic lower limb prosthesis design through simultaneous computer optimizations of human and prosthesis costs". *Scientific Reports*, **6**(1), Feb., p. 19983.
- [8] Gordon, D. F. N., Matsubara, T., Noda, T., Teramae, T., Morimoto, J., and Vijayakumar, S., 2018. "Bayesian Optimisation of Exoskeleton Design Parameters". In 2018 7th IEEE International Conference on Biomedical Robotics and Biomechatronics (Biorob), pp. 653–658.
- [9] Chen, B., Zi, B., Qin, L., and Pan, Q., 2020. "State-of-the-art research in robotic hip exoskeletons: A general review". *Journal of Orthopaedic Translation*, **20**, pp. 4–13.
- [10] Han, H., Wang, W., Zhang, F., Li, X., Chen, J., Han, J., and Zhang, J., 2021. "Selection of Muscle-Activity-Based Cost Function in Human-in-the-Loop Optimization of Multi-Gait Ankle Exoskeleton Assistance.". *IEEE transactions on neural systems and rehabilitation engineering : a publication of the IEEE Engineering in Medicine and Biology Society*, **29**, pp. 944–952. Place: United States.

- [11] Lorenz, R., Monti, R. P., Violante, I. R., Anagnostopoulos, C., Faisal, A. A., Montana, G., and Leech, R., 2016. “The Automatic Neuroscientist: A framework for optimizing experimental design with closed-loop real-time fMRI”. *NeuroImage*, **129**, pp. 320–334.
- [12] Kim, M., Ding, Y., Malcolm, P., Speeckaert, J., Sivi, C. J., Walsh, C. J., and Kuindersma, S., 2017. “Human-in-the-loop Bayesian optimization of wearable device parameters”. *PLOS ONE*, **12**(9), Sept., pp. 1–15. Publisher: Public Library of Science.
- [13] Makin, T. R., de Vignemont, F., and Faisal, A. A., 2017. “Neurocognitive barriers to the embodiment of technology”. *Nature Biomedical Engineering*, **1**(1), Jan., p. 0014.
- [14] Gordon, K. E., and Ferris, D. P., 2007. “Learning to walk with a robotic ankle exoskeleton”. *Journal of Biomechanics*, **40**(12), pp. 2636–2644.
- [15] Rosen, J., Brand, M., Fuchs, M., and Arcan, M., 2001. “A myosignal-based powered exoskeleton system”. *IEEE Transactions on Systems, Man, and Cybernetics - Part A: Systems and Humans*, **31**(3), pp. 210–222.
- [16] Fleischer, C., Reinicke, C., and Hommel, G., 2005. “Predicting the intended motion with EMG signals for an exoskeleton orthosis controller”. In 2005 IEEE/RSJ International Conference on Intelligent Robots and Systems, pp. 2029–2034.
- [17] Ren, P., Wang, W., Jing, Z., Chen, J., and Zhang, J., 2019. “Improving the Time Efficiency of sEMG-based Human-in-the-Loop Optimization”. In 2019 Chinese Control Conference (CCC), pp. 4626–4631.
- [18] Huang, H., Zhang, F., Hargrove, L. J., Dou, Z., Rogers, D. R., and Englehart, K. B., 2011. “Continuous locomotion-mode identification for prosthetic legs based on neuromuscular-mechanical fusion.”. *IEEE transactions on bio-medical engineering*, **58**(10), Oct., pp. 2867–2875. Place: United States.
- [19] Kantharaju, P., Jeong, H., Ramadurai, S., Jacobson, M., Jeong, H., and Kim, M., 2022. “Reducing squat physical effort using personalized assistance from an ankle exoskeleton”. *IEEE Transactions on Neural Systems and Rehabilitation Engineering*, **30**, pp. 1786–1795.
- [20] Akima, H., 1991. “A method of univariate interpolation that has the accuracy of a third-degree polynomial”. *ACM Transactions on Mathematical Software (TOMS)*, **17**(3), pp. 341–366.
- [21] Koller, J. R., Gates, D. H., Ferris, D. P., and Remy, C. D., 2016. “Confidence in the curve: Establishing instantaneous cost mapping”.